Additive Manufacturing 32 (2020) 101108

Contents lists available at ScienceDirect

Additive Manufacturing

journal homepage: www.elsevier.com/locate/addma

Full Length Article

Hybrid parts produced by deposition of 18Ni300 maraging steel via selective laser melting on forged and heat treated advanced high strength steel

Ludmila Kučerová*, Ivana Zetková, Štěpán Jeníček, Karolína Burdová

Regional Technological Institute, University of West Bohemia, Univerzitni 8, 30614, Plzen, Czech Republic

ARTICLE INFO

Keywords:
Powder bed fusion
Selective laser melting
Hybrid part
Maraging steel
Advanced high strength steel

ABSTRACT

Long production times, the associated high costs of the products and product size limitations belong among current issues of selective laser melting (SLM) technology. Hybrid products containing small and complex-shaped parts deposited by SLM on the forged, rolled or hot stamped semi-products could offer a practical solution to these limitations. Cylindrical hybrid parts were additively manufactured by depositing 18Ni300 maraging steel on the cylindrical semi-products of CMnAlNb low-alloy advanced high strength steel (AHSS). The AHSS was used either in forged and air cooled condition or after heat treatments typically used for inducing the TRIP (transformation induced plasticity) effect. Various post-build heat treatments of the hybrid parts were performed. The mechanical properties of the hybrid parts were determined by hardness measurement across the interface and by a tensile test of the dissimilar joints. All tensile samples fractured in the high-strength steel side, several millimetres from the interface. Microstructure analysis of both materials and the interface region was carried out using light and scanning electron microscopes. The hybrid parts had the ultimate tensile strengths of 840 – 940 MPa, with total elongations of 12–19 %. The best combination of tensile strength and elongation was obtained with two-step heat treatment of the TRIP steel prior to additive manufacturing with no post-build heat treatment of the hybrid part.

1. Introduction

Selective laser melting (SLM) is one of the additive manufacturing (AM) methods. As a rapidly advancing and expanding technique, it has been drawing the attention of researchers [1–7]. SLM is a powder bed process where laser beam melts and consolidates defined layers of powder together. Various metals are processed, ranging from aluminium alloys, tool and stainless steels to titanium alloys [8–11].

Among maraging steels for additive manufacturing, the Ni-Co-Mo-alloyed 1.2709 steel is one of the most widely-used ones. Intensive investigations are therefore underway into the effects of additive manufacturing per se [2,4,12,13], the building orientation [6,14] and the post-build heat treatments [7,15,16] on its microstructure and mechanical properties. Following the development of equipment and methods of additive manufacturing, in-situ alloying or variations of alloy contents were designed and produced. Powder-bed based AM technologies are considered unsuitable for making compositionally graded materials, especially as welding of incompatible materials results in poor bonding strength at the interface between two materials [17]. Bi-metallic (mainly Ti alloy containing systems) and metal-ceramic compositionally graded materials have been therefore produced mainly by direct energy deposition or powder bed fusion technologies [17–22].

Lately, in an effort to expand the application potential of the relatively new AM field, several studies discussed the possibility of incorporating AM into complex conventional production chains [23–25]. There have been some attempts recently to join two steels produced by additive manufacturing or to produce hybrid parts by depositing material by additive manufacturing onto conventionally-processed forgings or castings [26–28]. Successful AM deposition of 18Ni300 maraging steel onto substrates of conventional maraging steel of the same composition, H13 tool steel, and AISI 420 steel has been reported recently [29–31]. Still, only a few combinations of materials have been tested and reported so far. There is certainly a need for further works on this topic. Major drawbacks of metal additive manufacturing include long production times, the associated high costs of the products, and product size limitations imposed by typical sizes of build chambers. Additive manufacturing of small and complex-shaped details on forgings, rolled or hot stamped parts would, therefore, address the above issues and pave the way for new applications. As-built or solution-annealed 18Ni300 steel can reach strengths of around 1000 MPa which makes it a candidate for the production of hybrid parts in combination

* Corresponding author.
E-mail address: skalova.lida@seznam.cz (L. Kučerová).

https://doi.org/10.1016/j.addma.2020.101108
Received 23 November 2019; Received in revised form 3 February 2020; Accepted 3 February 2020
Available online 03 February 2020

with first-generation high strength steels [32–34].

In the present article, CMnAlNb low-carbon low-alloyed TRIP (transformation induced plasticity) steel was used as a semi-product for AM deposition of maraging steel. TRIP steels belong to the first generation of advanced high strength steels (AHSS) with relatively high strengths of 800 − 900 MPa and total elongations near 30 % [32,33]. These good mechanical properties result from the strain-induced transformation of metastable retained austenite into martensite under cold plastic deformation. When the distribution and morphology of and carbon content in retained austenite are favourable, austenitic grains and laths have different degrees of stability against martensitic transformation. Martensitic transformation than occurs gradually during straining and delays the onset of necking [29]. The region of uniform plastic deformation is therefore extended. Consequently, TRIP steels possess good deep drawing ability, which makes them suitable for applications in the automotive industry. In order to attain the desired mechanical and technological properties, TRIP steels undergo special heat treatment or thermo-mechanical treatment. It produces multiphase microstructures consisting of bainite, ferrite and retained austenite. Isothermal holding in the temperature interval of bainitic transformation is the typical feature of TRIP steel processing [35–37], although successful trials involving continuous cooling have been reported [38,39]. One of the main weaknesses of TRIP steels concerns their joints with similar and dissimilar materials. The weldability of conventional high-silicon TRIP steels is rather limited [40–43]. One of the successful joining methods is laser welding [44]. This study explores the ability to produce dissimilar joints by direct deposition of maraging steel on a TRIP steel cylindrical semi-product by the SLM process and the characteristics of the interface between these two materials.

2. Materials and methods

2.1. Materials

A low-carbon low-alloy steel (Table 1) with a chemical composition facilitating the TRIP effect was chosen as the conventional semi-product for creating a hybrid part. The steel is alloyed with Mn, which contributes to the stabilization of retained austenite. The first generation of TRIP steels contained around 1–2 % silicon, an element that prevents cementite formation during treatment and provides solid solution strengthening. However, these silicon levels led to surface quality problems in hot-dip galvanizing, and therefore alternative chemistries were sought. In the present steel, some silicon was substituted with aluminium, which also hinders cementite precipitation and provides solid solution strengthening [45]. Silicon, however, delivers stronger effects at the same alloying contents, which means that full substitution with aluminium could undesirably impair mechanical properties. Microalloying with niobium expands the processing parameter window and allows slower cooling of the steel without the risk of pearlite formation [33,46].

The steel was cast in an induction vacuum furnace. The ingot was cut into four equal parts and forged at 1150 °C into bars with a diameter of approximately 25 mm. The bars were air cooled and used for making samples for heat treatment and additive manufacturing. Some were used directly in as-hot forged and air cooled condition. Others underwent an additional full two stage heat treatment for TRIP steel. The as-forged microstructure consisted of pearlite and ferrite and rare islands of bainite, while two step heat treatment resulted in predominantly bainitic microstructure with retained austenite and a very small amount of proeutectoid ferrite.

Table 1
Chemical composition of the materials studied (weight %).

	C	Mn	Si	Cr	Ni	Mo	Ti	Co	Al	Nb
18Ni300	0.001	0.02	0.02	–	17.7	4.9	0.84	8.72	–	–
CMnAlNb	0.21	1.5	0.55	0.18	0.08	–	–	–	1.43	0.06

The material for additive manufacturing was 18Ni300 maraging steel. This steel is also known as X3NiCoMoTi 18-9-5, an equivalent to 1.2709 steel. The powder of this steel was supplied by EOS under the commercial name MS1. The average powder particle size was 25 µm. This steel was chosen because its mechanical properties are similar to those of the used TRIP steel. In the as-built condition, its strength is about 1100 MPa and elongation reaches 12 %. Post processing heat treatment is recommended to relieve the residual stresses generated by rapid heating and cooling involved in the AM process. Annealing at 820 °C – 900 °C relieves residual stresses and homogenizes the distribution of alloying elements. It slightly improves elongation to approximately 14 %, at the cost of a minor decrease in tensile strength by 50 − 100 MPa [14,23].

2.2. Processing

Cylinders 10 mm in diameter and 45 mm in length were made of CMnAlNb steel. On one end, they were provided with a machined thread to be screwed into a base plate (Fig. 1). On the other flat end, selective laser melting of MS1 steel was carried out to produce a cylindrical extension of the same diameter, i.e. 10 mm, and 30 mm in length.

The base plate and the faces of the samples should be high-quality planar surfaces for the first layer to be deposited to the achievable accuracy which is around half the thickness of the layer; in this case 0.02 mm. It is very important that both parts of the hybrid build are axially aligned.

The additive manufacturing process was carried out in the EOS M290 machine, using parameters recommended for tool steels: laser power of 258 W, the scanning rate of 960 m/s and layer thickness of 40 µm. A protective atmosphere of nitrogen gas was used to prevent oxidation in the process. The subsequent heat treatment was carried out in an argon atmosphere.

The deposition on the top face of round bars is governed by similar rules as an ordinary AM process on a base plate, the only difference being the absence of supporting structures. Conventionally, the first three layers of a build are usually printed with special parameters and comprise what is known as “down skin” (speed: 2400 mm/s, power: 145 W). In the case of this work, the down skin was not used, as the first layers were built directly on a solid material. The double melting of the first layer was carried out instead to secure a good bond between the bars and the build. The core of the build was created using standard “in fill” parameters (speed: 960 mm/s, power: 285 W). The last three layers were deposited using special parameters, making up the “up skin”. These parameters are specially adjusted to ensure that the upper surface of the build is of high quality. The whole surface of the build was formed using “contour” parameters (speed: 300 mm/s, power: 138 W). The purpose of the contour laser pass is to guarantee the shape and surface roughness of the part. The following constant parameters were used for all the above-described printing strategies: layer thickness of 0.04 mm, misorientation angle between two consecutive layers 67°, skipped layers = 0, offset layers = 0. Used misorientation angle is recommended by the printer supplier and it contributes to the high quality of printed parts. Skipped layer = 0 means, that every layer of the powder is melted (1 would mean that every second layer is melted etc.). Offset layer is an additional layer added to the exact dimensions of the desired product, typically for post-processing reasons. Offset layer = 0 means that no additional layer was printed.

Standard base plate from 1.2083 steel was used, however, it had been adjusted to provide stiffness in individual samples and minimize their thermal load from dissipated heat. The temperature of the base plate was 40 °C throughout the building process. For the sake of accuracy of the hybrid parts, centring pivots had to be produced to keep the base plate in an exact position in the machine. The most important for

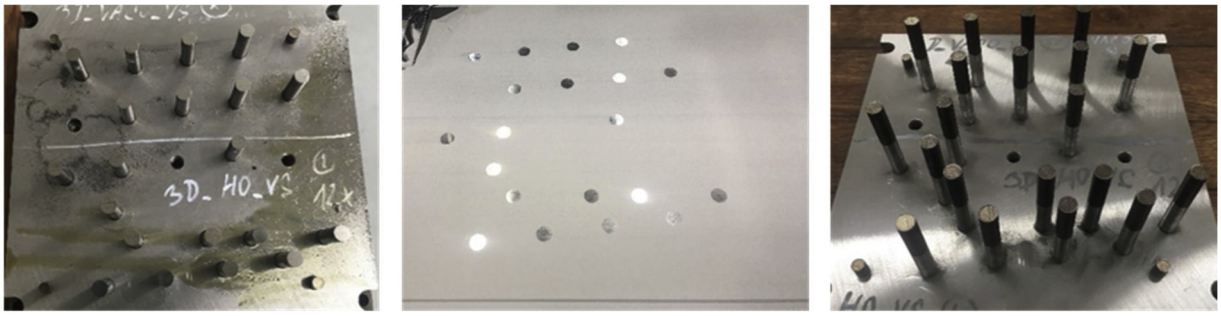

Fig. 1. a) AHSS CMnAlNb steel cylindrical samples on the base plate; b) the same base plate with samples embedded in powder, c) the final hybrid parts.

the successful processing of hybrid parts were precise data about the position of CMnAlNb cylindrical semi-products at the base plate. Therefore, cylinders of CMnAlNb steels were screwed into the base plate to ensure precise mounting. The height differences of mounted cylinders were in the region of hundredths of a millimetre and therefore the whole set up of a base plate with mounted cylinders had to be ground to obtain exactly the same height of the top bases of the cylinders. The base plate was then placed into a printing machine with top bases of the cylinders parallel to the edge of the recoater, to ensure the same thickness of the first layer for all samples. Due to this rather elaborate process the offset at the interface and thickens variations were negligible, well below the declared precision of the SLM method.

The low alloy CMnAlNb steel semi-product was used either in the forged and air cooled condition, which is further marked as "CMnAlNb without HT", or after an additional two-step heat treatment optimized for TRIP steels (Fig. 2, Table 2). The treatment consisted of heating to 900 °C, holding for 20 min, and cooling to an isothermal holding temperature at 425 °C. Cooling in a salt bath at 400 °C provided an average cooling rate of approx. 15 °C/s at the present sample size. Once the sample reached 425 °C, it was moved from the salt bath to a furnace at 425 °C and held for 20 min, and then air cooled to room temperature (sample 5 and sample 6).

This two-step TRIP treatment was also applied to two hybrid parts of CMnAlNb steel in the forged and air cooled state and AM maraging steel. In this case, both materials underwent the same heat treatment and two variations of the treatment were tested, with either 20 min (sample 3) or 60 min holds at 425 °C (sample 4).

To explore the effect of controlled cooling and isothermal holding, one hybrid part was soaked at 900 °C for 20 min, and then air cooled to room temperature (sample 2). This soaking temperature was chosen with reference to the 820 – 940 °C interval of typical solution annealing temperatures for the additive- manufactured 18Ni300 maraging steel. It is also a suitable soaking temperature for CMnAlNb steel [45]. The aim of various combinations of pre-treatment of CMnAlNb steel and post-build heat treatment of the whole hybrid part was to optimize the mechanical properties of the hybrid part. Therefore, intensive precipitation strengthening of the maraging steel to the tensile strengths around 2000 MPa is not desirable in this case, as the typical strength of low-alloy CMnAlNb does not exceed 1000 MPa.

2.3. Characterisation

The original microstructure of forged and annealed bars of CMnAlNb steel and maraging steel powder were documented using a light microscope and scanning electron microscope (SEM). Longitudinal metallographic sections (parallel to the axis of the hybrid parts) were prepared by standard procedures. Microstructures in hybrid parts were analysed using a Zeiss EVO 25 scanning electron microscope with a LaB6 cathode, a Zeiss Crossbeam microscope with a FEG cathode and a BX61 Olympus light microscope. The interface between the different steels was examined thoroughly as well.

Longitudinal metallographic sections from fractured tensile test samples were prepared in order to determine the relative position of the fracture to the CMnAlNb/maraging steel interface. The fracture surface morphology and type were identified using a scanning electron microscope. The metallographic samples of CMnAlNb steel and as-printed maraging steel were etched with 3 % nital. Samples of heat-treated maraging steel were etched with aqua regia to reveal microstructure features for observation at higher magnifications. If not indicated otherwise, the micrographs below show the core of the builds, where the defined angle between the laser tracks in consecutive layers was 67°.

The amount of retained austenite was measured by X-ray diffraction using an AXS Bruker D8 Discover automatic powder diffractometer with a HI-STAR detector and a Co lamp ($\lambda K\alpha$ = 0.1790307 nm). A focusing polycapillary lens was deployed to produce an X-ray spot with a 0.5 mm diameter. The measured location was in the central portion of the samples. Spectra were taken in the range of 2 ϑ from 25° to 110°. The integrated intensities of (200) ferrite peak and (111), (002) and (022) austenite peaks were used for evaluating volume fractions of ferrite and retained austenite.

Hardness HV10 was measured using a Wolpert 432-SVD instrument as an indication of the mechanical properties of both steels after various heat treatments. Line profiles of microhardness HV0.1 across the interface between the materials were taken using a UHL VMH-002 V instrument. The length of the line segment was 2 mm, with the interface being in the middle. The imprints were spaced at 0.1 mm. Hardness and microhardness were measured at polished metallographic sections.

Small cylindrical tensile samples were machined, with a gauge

Fig. 2. Processing route with heat treatment combinations for used hybrid parts.

Table 2
Heat treatment conditions of individual samples.

Sample title	Heat treatment of forged AHSS before AM	Post-build heat treatment of hybrid part after AM
1 – CMnAlNb without HT, no post-build HT	Without heat treatment	Without heat treatment
2 – CMnAlNb without HT, post-build annealed at 900 °C	Without heat treatment	900 °C/20 min, air cooling
3 – CMnAlNb without HT, post-build two-step HT 900 °C/20 min, 425 °C/ 20 min	Without heat treatment	900 °C/20 min, 425 °C/20 min
4 – CMnAlNb without HT, post-build two-step HT 900 °C/20 min, 425 °C/ 60 min	Without heat treatment	900 °C/20 min, 425 °C/ 60 min
5 – CMnAlNb 900 °C/20 min - 425 °C/20 min, no post-build HT	900 °C/20 min, 425 °C/20 min	Without heat treatment
6 - CMnAlNb 900 °C/20 min - 425 °C/20 min, post-build annealed 200 °C/ 120 min	900 °C/20 min, 425 °C /20 min	200 °C/120 min

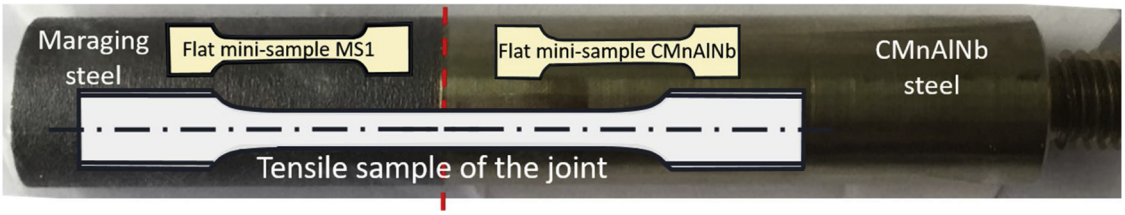

Fig. 3. Positions of tensile samples within a hybrid part.

diameter of 4 mm, gauge length of 20 mm and an M8-threaded head. The interface between the materials was in the central portion of the gauge length (Fig. 3). Testing was performed at room temperature. Results in the form of average values and standard deviations are given in Table 2. To compare mechanical properties after different heat treatments in each steel, two sub-sized flat samples of homogeneous material was made from each side of a hybrid product. These samples had a cross-section of 2 × 1.2 mm and a gauge length of 5 mm. The testing procedure was carried out in a Zwick Roller Z250 testing machine and followed EN ISO 6892-1, with a strain rate of 0.0067 s^{-1}.

3. Results and discussion

3.1. Microstructure

The first hybrid part received no post processing heat treatment. The maraging steel contained a cell-type microstructure (Fig. 4a, Fig. 5a), which is typical of additive-manufactured maraging steel [7]. This very fine microstructure results from extremely high temperature gradients that exist during additive manufacturing. The gradients also caused non-uniform distribution of alloying elements, which segregated along cell boundaries. CMnAlNb steel contained a ferritic-bainitic-pearlitic microstructure with a significant amount of polygonal ferrite (Fig. 6a. Fig. 7a). There was about 5 % of retained austenite in the maraging steel and no retained austenite in the CMnAlNb steel (Table 2).

In large samples that included the interface and were taken from the builds heat-treated at 900 °C, which was aimed at homogenization and stress relief, both materials underwent the post-build heat treatment. The microstructure of maraging steel corresponds to solution annealed builds of maraging steel [7]. In this sample, the original cell-type microstructure has dissolved, as the alloying elements were redistributed more evenly. The microstructure consisted of martensite plates (Fig. 4b, Fig. 5b). Retained austenite was eliminated by annealing. The boundaries of laser beam tracks were still distinguishable in light micrographs and in some scanning electron micrographs. After this heat treatment, the microstructure of CMnAlNb steel consisted of a mixture of various types and morphologies of bainite, ferrite and a small amount of pearlite (Fig. 6b). The microstructure contained bands of coarse bainite sheaves and bands of granular bainite with laths and islands of retained austenite dispersed within a ferritic matrix (Fig. 7b).

After the two-step heat treatment with the shorter 20 min hold at 425 °C, the microstructure of the maraging steel was similar to that after simple annealing. It consisted of rather coarse martensite laths with particles (Fig. 4c, Fig. 5c). The microstructure of CMnAlNb TRIP steel was predominantly bainitic with approximately 11 % retained austenite (Fig. 6c). Bainite had a lath form. Its islands were embedded in very thin austenite films or laths, which formed rather smooth enclosed regions. Bainite laths were denser and thinner than in forged and annealed samples (Fig. 7c). Retained austenite was not detected in maraging steel after this treatment.

Two-step post-build heat treatment with the longer 60 min hold at 425 °C led to similar microstructures in both steels. The maraging steel contained martensite with evenly-distributed Ni_3Ti and Ni_3(Ti, Mo) particles (Fig. 4d, Fig. 5d). CMnAlNb steel had, again, bainitic microstructure with a predominantly lath morphology (Fig. 6d). The bainite laths were finer than in the sample after the 20 min hold; in addition, there was less bainitic ferrite. Fine islands of retained austenite were found at the boundaries of bainite blocks (Fig. 7d). The volume fraction of retained austenite, 13 %, was slightly higher than in the sample which underwent the shorter hold. No retained austenite was found in maraging steel.

It is interesting to note that the final microstructure of CMnAlNb after pre-build two-step heat treatment with a 20 min hold at 425 °C was different from the microstructure of CMnAlNb which underwent this heat treatment only after the additive manufacturing process (Fig. 6e). The microstructure was still bainite-dominated but the areas of bainitic ferrite were generally larger and prevailed more strongly over the other phases. The amount of bainitic ferrite was larger, and it was a dominant phase in the bainite (Fig. 7e). Bainite was predominantly granular, complemented with scattered lath bainite. This microstructure contained the largest amount of retained austenite (15 %). Since no post processing was applied to this hybrid part, maraging steel had an as-printed cell microstructure (Fig. 4e, Fig. 5e).

Application of 120 min annealing at 200 °C to a hybrid part made with CMnAlNb which had been heat-treated in two steps with a 20 min hold at 425 °C prior to AM, resulted in little changes to the microstructure of CMnAlNb steel (Fig. 6f, Fig. 7f). In the maraging steel, the cell boundaries seemed to be more distinctive after the annealing than in the as-built state (Fig. 4f, Fig. 5f). No other visible changes were found.

For all combinations of prior and post-build heat treatments, the interface between the conventional and the AM material displays no porosity or lack of fusion and shows a very complex arrangement – in

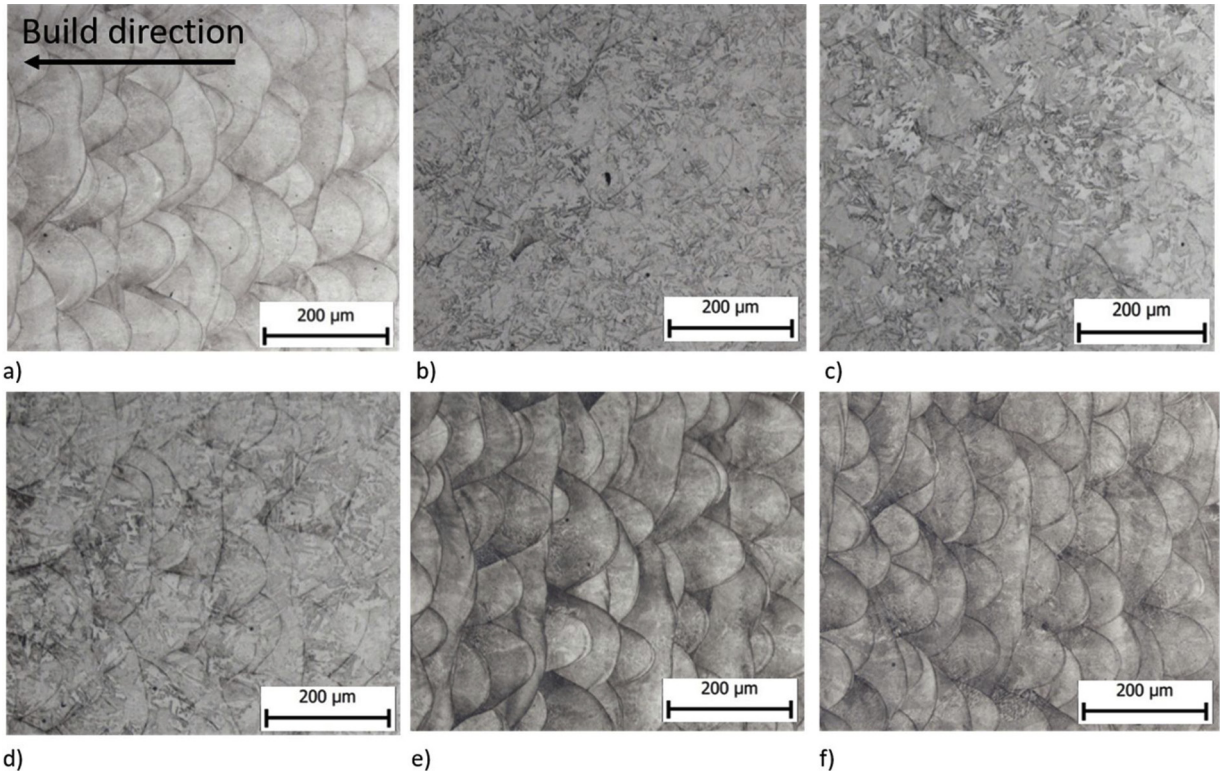

Fig. 4. Light micrographs of maraging steel, build direction was the same for all the images, description of heat treatment of maraging steel only is given: a) sample 1 - no post-build treatment, b) sample 2 – solution-annealed at 900 °C, c) sample 3 – two-step HT 900 °C/20 min, 425 °C/20 min, d) sample 4 - two-step HT 900 °C/20 min, 425 °C/60 min, e) sample 5 - no post-build treatment, f) sample 6 - annealed at 200 °C/120 min.

both materials (Fig. 8). The interface does not follow the original surface of the cylinder from advanced high strength CMnAlNb steel. Instead, the mixed material from the surface and maraging steel extend into CMnAlNb steel, forming typical shapes. Strips of very fine bainite are found within the cell-type microstructure of maraging steel (Fig. 8a, b). It became apparent that the laser beam re-melted the very surface of the CMnAlNb steel, creating a cell-like microstructure on the side of the high strength steel as well (Fig. 8c). The microstructure of the CMnAlNb steel at the interface does not at all resemble the microstructures found in fusion zones of welds in these steels [47], as those tend to contain conventional martensitic or martensitic-bainitic microstructures. A local analysis of chemical composition by EDS revealed that concentrations of alloying elements vary significantly between neighbouring regions (Fig. 9a-c). Nickel and cobalt distributions are

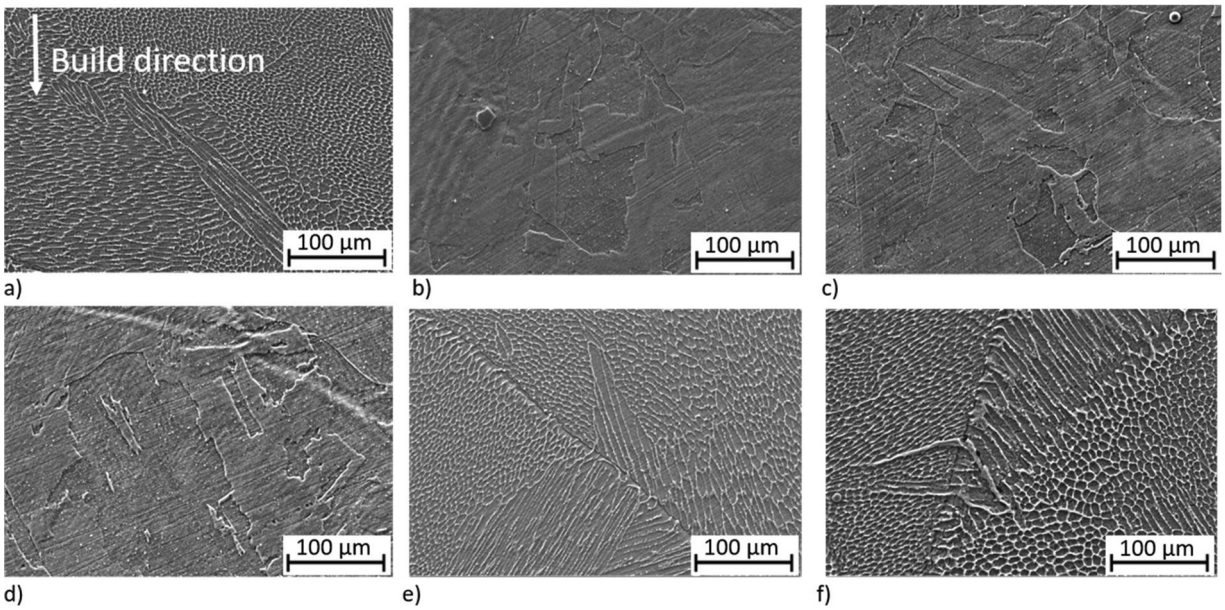

Fig. 5. Scanning electron micrographs of maraging steel, build direction was the same for all the images, description of heat treatment of maraging steel only is given: a) sample 1 - no post-build treatment, b) sample 2 – solution-annealed at 900 °C, c) sample 3 – two-step HT 900 °C/20 min, 425 °C/20 min, d) sample 4 – two-step HT 900 °C/20 min, 425 °C/60 min, e) sample 5 - no post processing, f) sample 6 - annealed at 200 °C/120 min.

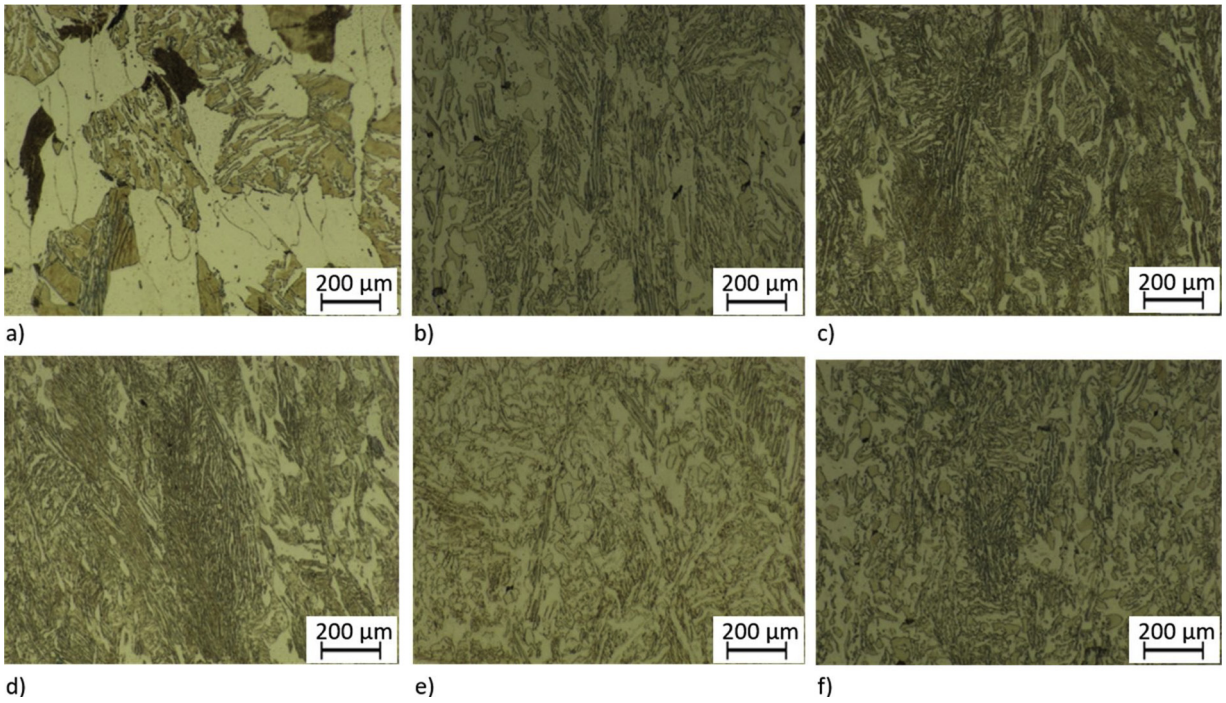

Fig. 6. Light micrographs of CMnAlNb steel: a) sample 1 - forged and air cooled, b) sample 2 – solution-annealed at 900 °C/20 min, c) sample 3 - two-step post-build HT 900 °C/20 min, 425 °C/20 min, d) sample 4 – two-step post-build HT 900 °C/20 min, 425 °C/60 min, e) sample 5 – two-step HT 900 °C/20 min, 425 °C/20 min prior to additive manufacturing, no post-build treatment, f) sample 6 – two-step HT 900 °C/20 min, 425 °C/20 min prior to additive manufacturing, post-process annealed at 200 °C/120 min.

particularly telling examples of these variations (Fig. 9c). The aluminium level is gradually decreasing across the interface, but not quite at the same rate as Ni and Co.

3.2. Mechanical properties

3.2.1. Measurement of hardness and microhardness

Line profiles of micro-hardness were measured at metallographic sections, starting on the maraging steel side, approximately 1 mm from the interface. The hardness of maraging steel in the as-built condition (samples 1 and 5) is very similar to hardness levels in most of the other samples: approximately 370 HV (Fig. 10). The two-step post-build heat treatment (samples 3 and 4) and post-build annealing (sample 2) were the procedures that resulted in the softening of maraging steel to 300 HV. The same softening was reported for additive-manufactured maraging steel solution-treated at 820 °C for 20 min [7], where

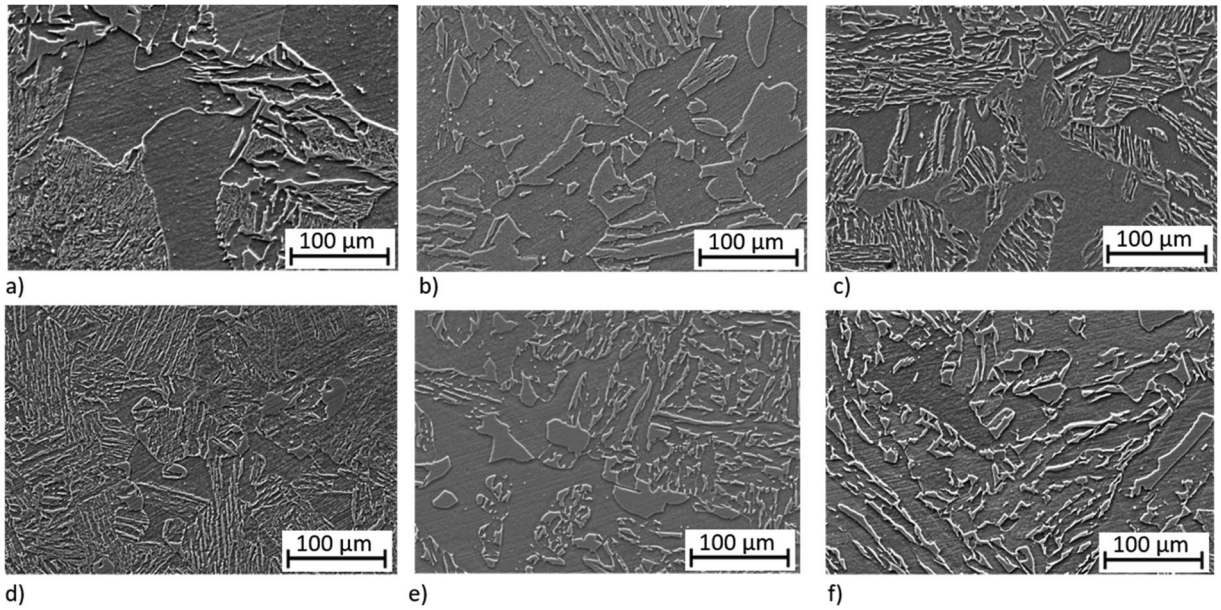

Fig. 7. Scanning electron micrographs of CMnAlNb steel: a) sample 1 - forged and air cooled, b) sample 2 – solution-annealed at 900 °C/20 min, c) sample 3 – two-step post-build HT 900 °C/20 min, 425 °C/20 min, d) sample 4 – two-step post-build HT 900 °C/20 min, 425 °C/60 min, e) sample 5 – two-step HT 900 °C/20 min, 425 °C/20 min prior to additive manufacturing, no post-build treatment, f) sample 6 – two-step HT 900 °C/20 min, 425 °C/20 min prior to additive manufacturing, and post-build annealing at 200 °C/120 min.

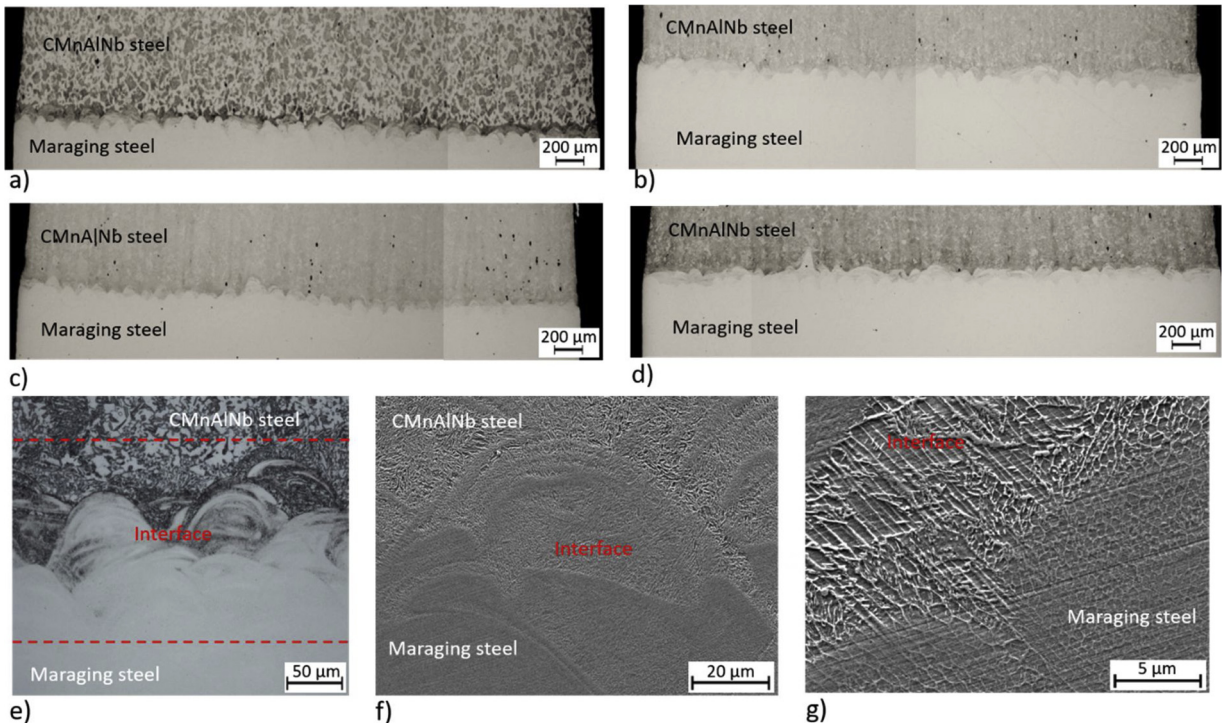

Fig. 8. Macro views of interface between CMnAlNb AHSS and maraging steel a) sample 1 – CMnAlNb without HT, no post-build HT, b) sample 3 – CMnAlNb without HT, post-build two-step HT 900 °C/20 min, 425 °C/20 min, c) sample CMnAlNb 900 °C/20 min - 425 °C/20 min, no post-build HT, d) sample - CMnAlNb 900 °C/20 min - 425 °C/20 min, post-build annealed 200 °C/120 min. The microstructure at this interface is shown at increasing magnifications from e) to g).

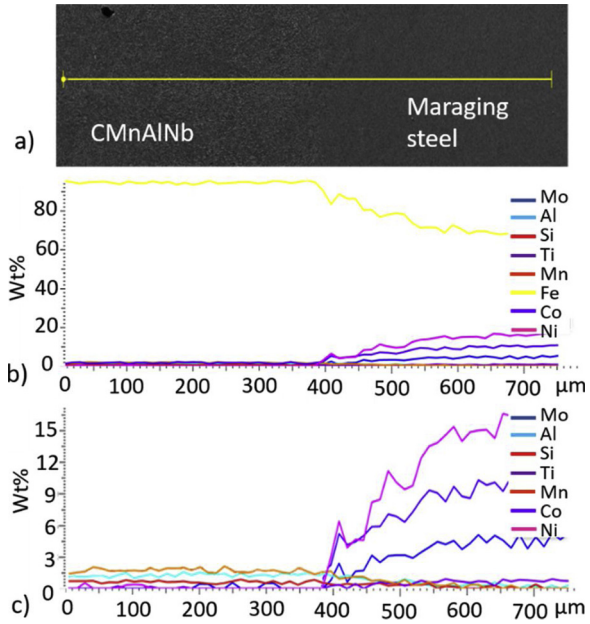

Fig. 9. Change in alloying element levels across the interface: a) line scan area b) distribution of alloying elements across the interface, c) detail of distribution of alloying elements present in lower contents (without Fe).

hardness dropped by around 50 points HV. The recommended solution annealing procedures for this steel range from 820 °C/20 min, an earlier recommendation by the manufacturer, to 940 °C/120 min, a current recommendation, followed by slow cooling to room temperature. The temperature of 900 °C which is used in all the sequences in the present study was between the old and the new recommended temperatures. One can, therefore, expect that softening due to stress relief, and chemical homogenization, could be more effective than at 820 °C. It is also interesting to note that neither the cooling rate nor the presence/absence of a hold at 425 °C had any measurable effect on the hardness of the maraging steel. Not even the sample which had been held at 425 °C for one hour showed any signs of precipitation hardening. The recommended precipitation hardening treatment for this steel is a 6 -h hold at 480 °C. Some researchers, however, reported the clustering of solutes with a hardening effect after very short holding at this temperature [15]. As was already noted, intensive precipitation strengthening of the maraging steel was not required in this case. Maximizing the precipitation strengthening potential of maraging steel would double its hardness and tensile strength in comparison to an annealed state, creating a large difference between the mechanical properties of CMnAlNb steel and maraging steel.

Forged CMnAlNb steel without heat treatment (sample 1) had a relatively low hardness: about 230 HV10. The large scatter in microhardness values can be attributed to the presence of microstructure constituents with disparate mechanical properties, such as ferrite and pearlite. These constituents were strongly banded. Consequently, the measured value depended on the location of the imprint – in a ferrite or pearlite band. The heat treatment with continuous cooling did not affect hardness values to any significant extent. The two-step TRIP treatment, however, produced a hardness above 300 HV (sample 3). After the longer annealing at 425 °C, the hardness decreased slightly (sample 4).

Hardness values changed dramatically within a very short distance on the CMnAlNb side. The gradient on the side of the maraging steel, however, was less steep. Both samples of hybrid parts after TRIP treatment showed local softening on the CMnAlNb side of the interface. The largest amount of softening was found after the heat treatment that involved the longer hold at 425 °C (sample 4). This softening behaviour due to local tempering was also observed in welds of low-alloy TRIP steel [48], where it was most notable after arc welding but hardly noticeable after laser welding. As in the case of laser-welded (and opposed to arc-welded) TRIP steel, only mild tempering occurred and no carbide precipitation was observed in the softened area of hybrid samples in

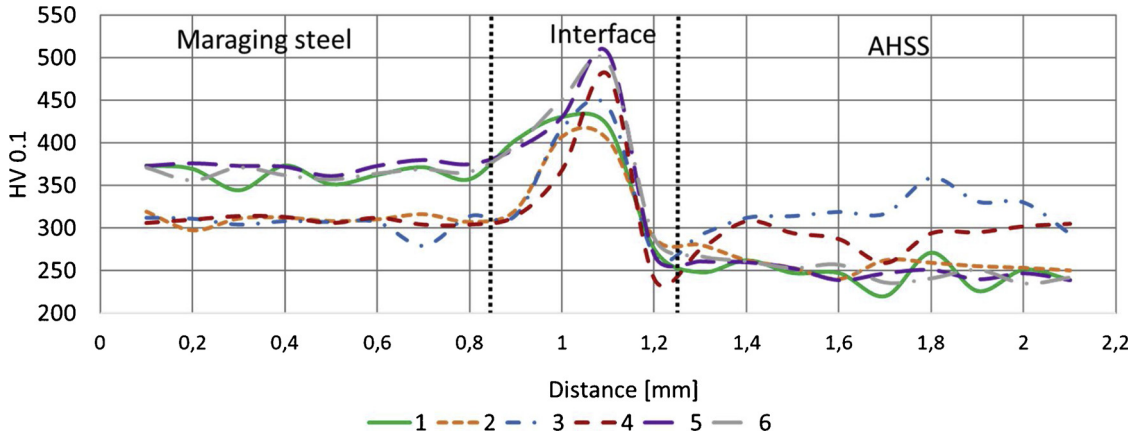

Fig. 10. Microhardness profile across the interface, measured from maraging steel to CMnAlNb AHSS steel side. Heat treatment sequences of hybrid samples: 1 – CMnAlNb without HT, no post-build HT, 2 – CMnAlNb without HT, post-build annealed at 900 °C, 3 – CMnAlNb without HT, post-build two-step HT 900 °C/20 min, 425 °C/20 min, 4 – CMnAlNb without HT, post-build two-step HT 900 °C/20 min, 425 °C/60 min, 5 – CMnAlNb 900 °C/20 min - 425 °C/20 min, no post-build HT, 6 - CMnAlNb 900 °C/20 min - 425 °C/20 min, post-build annealed 200 °C/120 min.

scanning electron micrographs.

The interface region, which can be seen as equivalent to fusion and heat-affected zones in conventional welds, was approximately 380 µm in width in all hybrid samples, as identified from the hardness profile (Fig. 10). About the same width was found from the distribution of alloying elements. Changes in the microstructure were visible within around 170 µm wide area around the interface. A similar heat-affected zone with a smaller thickness of 200 µm was reported in MS1-H13 hybrid joints [29].

3.2.2. Tensile testing

Two tensile test geometries were used in this experiment. The larger samples contained the maraging steel – high-strength steel interface in the middle of the gauge length. They were used to characterise the properties of the entire hybrid part. Sub-size flat samples were prepared from the maraging steel and CMnAlNb steel sides. Due to different sample geometries, the properties cannot be compared directly between the two specimen types. Generally, shorter specimens tend to give higher elongations for ductile materials, as the necking deformation is evaluated across a shorter gauge length L_0. Strengths are considered to be comparable between samples of different geometries, although it may not apply to additively-manufactured steels. The smaller the cross-section of sub-size flat samples is, the lower is the number of melted layers on the cross-section, which makes the adverse effect of any melting defect more significant. Hence, smaller tensile samples are likely to exhibit lower yield and tensile strengths. Still, the mechanical properties determined using sub-sized samples can be useful for assessing the changes in CMnAlNb steel and maraging steel induced by different heat treatments. All sub-size samples were taken from hybrid parts after post-process heat treatment and therefore, they do not provide information on the mechanical properties of CMnAlNb steel prior to additive manufacturing.

The hybrid part without post-build heat treatment (sample 1) had a yield tensile strength (YTS) of 502 MPa, a good ultimate tensile strength (UTS) of 841 MPa and a total elongation of 12 % (Table 3). Considering that CMnAlNb steel in this hybrid part only had a yield strength of 385 MPa and a tensile strength of 719 MPa, it means that the properties of the dissimilar joint were improved thanks to the AM maraging steel with YTS of 738 MPa and UTS of 902 MPa. The total elongation in the hybrid part was much lower than in either steel but the different sample geometries need to be considered. Sub-sized flat samples tend to yield higher elongation values. 12 % elongation is a normal value in larger tensile specimens of as-built maraging steel [7,14].

In a post-build solution-annealed hybrid part (sample 2), the tensile strengths of both steels slightly increased, as well as the total elongation of CMnAlNb steel. The sample which included the interface also had a higher tensile strength: 899 MPa, along with 16 % elongation, and uniform plastic deformation (Ag) which increased from 7 to 9 %.

Two hybrid parts received two-step TRIP heat treatment (sample 3 and sample 4). The large sample from the part held at 425 °C for 20 min (sample 3) showed an excellent strength of 942 MPa, a yield strength of 750 MPa and a total elongation of 14 %. This high strength in the hybrid part resulted from the higher tensile strength of CMnAlNb steel of 852 MPa and the yield strength of 650 MPa. The total elongation in CMnAlNb steel alone was nearly the same as in the previous samples, reaching 32 %. However, the uniform plastic deformation dropped to 12 %. The tensile strength of maraging steel was slightly above 900 MPa, with the yield strength reduced to 738 MPa.

In another hybrid part (sample 4), holding at 425 °C for 60 min did not change the mechanical properties of the part. The mechanical properties of both materials were the same as those after the shorter hold. Microstructure observations confirm this finding. No significant precipitation hardening occurred as a result of the longer hold. To exclude any error on the side of the heat treatment procedure or mechanical testing, this treatment was repeated twice with the same results. The reason for repeating the procedure was that its results were in contrast with reported observations of precipitation behaviour in this maraging steel, either in as-built or solution-annealed condition, where the steel was cooled down to room temperature prior to precipitation hardening. The recommended precipitation hardening consists of holding at 490 °C for as long as 6 h. However, it was found that first clustering and precipitation occurred just several minutes into the hold at these temperatures [13] and minor hardening effects were found in as-built samples held for two hours at a mere 350 °C. Yin [15] reported that the tensile strength of printed samples held for 3 h at 390 °C increased from 1150 MPa to 1600 MPa. For the same 300-grade maraging steel solution-annealed at 840 °C for 1 h and precipitation-hardened at 490 °C for 6 h, Tan [5] reported that its hardness was just 1–2 HRC less than in the post-build hardened material and its UTS was just 50 MPa less at 1940 MPa. Similar results were reported by Bai [2]: annealing at 840 °C for 1 h followed by precipitation hardening at 480 °C for 6 h led to a hardness of 650 HV and an ultimate tensile strength of 2160 MPa. In all these studies, solution annealing and precipitation hardening were carried out as two separate operations. Hence, it appears that this lack of hardening behaviour is associated with annealing and precipitation-hardening combined in a single step, i.e. without cooling to room temperature between them. This finding would deserve further investigation.

The best total elongations of 19 % were achieved in those hybrid parts, in which the TRIP processing was applied to CMnAlNb prior to

Table 3
Mechanical properties of hybrid parts including the interface region (yield tensile strength (YTS), ultimate tensile strength (UTS), total elongation (A), uniform plastic elongation (Ag), retained austenite volume fraction (RA), Vickers hardness (HV10)). Mechanical properties of both steels (CMnAlNb and Maraging) after additive manufacturing and post-build treatment as determined from sub-size samples The number of a sample (No), heat treatment of CMnAlNb prior to additive manufacturing (Prior HT of CMnAlNb) and heat treatment of the AM hybrid part (HT of hybrid part after AM) are identified.

Sample No.	Prior HT of CMnAlNb	HT of hybrid part after AM	YTS [MPa]	UTS [MPa]	A [%]	Ag [%]	RA [%]	HV10 [-]
Hybrid part 1	Forged, no HT	No HT	502 ± 19	841 ± 26	12 ± 1	7 ± 1	–	–
CMnAlNb 1	Forged, no HT	No HT	385 ± 1	719 ± 1	30 ± 0	21 ± 0	0	223
Maraging 1	–	No HT	815 ± 5	955 ± 4	23 ± 1	2 ± 1	5	375
Hybrid part 2	Forged, no HT	900 °C/20 min, air cooling	472 ± 5	889 ± 12	16 ± 0	9 ± 0	–	–
CMnAlNb 2	Forged, no HT	900 °C/20 min, air cooling	374 ± 3	793 ± 5	34 ± 2	24 ± 0	0	239
Maraging 2	–	900 °C/20 min, air cooling	733 ± 3	911 ± 4	23 ± 1	2 ± 0	0	307
Hybrid part 3	Forged, no HT	900 °C/20 min, 425 °C/20 min	750 ± 19	942 ± 16	14 ± 1	4 ± 0	–	–
CMnAlNb 3	Forged, no HT	900 °C/20 min, 425 °C/20 min	650 ± 4	852 ± 1	32 ± 0	12 ± 0	11	304
Maraging 3	–	900 °C/20 min, 425 °C/20 min	738 ± 4	902 ± 0	23 ± 1	2 ± 0	2	307
Hybrid part 4	Forged, no HT	900 °C/20 min, 425 °C/ 60 min	753 ± 17	939 ± 17	15 ± 1	5 ± 0	–	–
CMnAlNb 4	Forged, no HT	900 °C/20 min, 425 °C/ 60 min	624 ± 12	824 ± 7	34 ± 0	15 ± 0	13	296
Maraging 4	–	900 °C/20 min, 425 °C/ 60 min	765 ± 4	901 ± 1	23 ± 0	2 ± 0	0	309
Hybrid part 5	900 °C/20 min, 425 °C/20 min	No HT	516 ± 36	862 ± 41	19 ± 2	10 ± 1	–	–
CMnAlNb 5	900 °C/20 min, 425 °C/20 min	No HT	458 ± 4	756 ± 12	50 ± 1	33 ± 0	15	245
Maraging 5	–	No HT	815 ± 5	955 ± 4	23 ± 1	2 ± 1	5	369
Hybrid part 6	900 °C/20 min, 425 °C /20 min	200 °C/120 min	525 ± 36	863 ± 25	19 ± 1	10 ± 0	–	–
CMnAlNb 6	900 °C/20 min, 425 °C /20 min	200 °C/120 min	412 ± 4	786 ± 4	44 ± 1	30 ± 0	18	235
Maraging 6	–	200 °C/120 min	958 ± 4	1077 ± 5	23 ± 1	3 ± 0	5	372

additive manufacturing (sample 5 and sample 6). The ultimate strengths of those hybrid parts were equal to the typical strengths of the TRIP steel. However, their elongation levels were lower, due to the limited ductility of the AM steel. Yet, uniform plastic elongation (up to the point of necking) was the highest of all the variants. Here, the amount of plasticity was larger than in other hybrid parts composed of as-built maraging steel and low carbon steel in different microstructural states. It can be assumed that this might result from a combined effect of activation of the TRIP effect and larger areas of soft bainitic ferrite.

A hybrid part after two-hour exposure at 200 °C was also tested (sample 6). This might be interesting in relation to the thermal stability of retained austenite and the TRIP effect in both steels. The relatively long annealing operation did not affect the microstructure in any detectable way. This post processing slightly reduced the strength of CMnAlNb steel. On the other hand, the ultimate tensile strength of maraging steel finally increased to 1077 MPa and its yield strength rose to 958 MPa, whereas total elongation has not changed. This suggests that some microstructural changes and precipitation have already started, even though they were not yet reflected in hardness values. No literature data were found for comparison, but another, a larger experimental programme is underway to test the precipitation behaviour of as-built maraging steel at these moderate temperatures.

The comparison between the properties of each steel alone and those of the hybrid parts reveals that the properties of the hybrid part were governed by the weaker CMnNb steel in all the samples. The total elongation and uniform plastic elongation in all the hybrid parts were higher than typical elongations of larger samples of this maraging steel after similar post processing [14]. Hence, a disproportionately large part of elongation had to be accommodated by the CMnAlNb steel side of the hybrid sample. All tensile samples also fractured in CMnAlNb steel, several millimetres from the interface.

The hybrid parts after two-step post-build heat treatment (sample 3 and sample 4) showed a different strengthening behaviour (Fig. 11) from the parts with no post-build treatment or upon solution annealing (sample 2 and 5). The first displayed rapid strengthening and short uniform plastic deformation until the onset of necking. This was also reflected in the tensile behaviour of the AHSS steel alone (Table 2). This behaviour could be connected to the mechanical properties of CMnAlNb steel, as the CMnAlNb steel sides of two hybrid parts (samples 3, 4) showed the lowest Ag values: 12 % and 15 %, respectively and the highest values of yield and ultimate strengths.

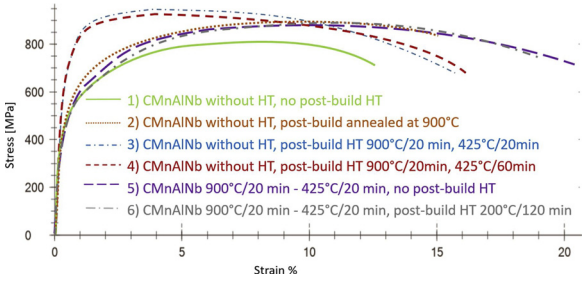

Fig. 11. Stress-strain curves of hybrid parts from tensile testing of cylindrical samples with the interface region in the middle of their gauge length.

3.2.3. *Fracture analysis*

The hardness and in turn strength of CMnAlNb steel was equal to or slightly lower than the hardness of maraging steel, regardless of the heat treatment procedure. Hardness was higher around the interface. The microcleanliness of the AM maraging steel was better than that of CMnAlNb steel, where the latter contained numerous coarse Al particles. This is in contrast to reports concerning other hybrid parts [29,30], where the AM steels had lower quality than their conventional counterparts, due to high porosity. Considering this, it should not be surprising that in all the samples in this study, failure occurred in CMnAlNb steel. The fracture was always located several millimetres from the CMnAlNb/maraging steel interface, which suggests that the interface and the adjacent heat-affected zone on the CMnAlNb side are not the weakest regions in these hybrid parts. This contradicts the results obtained for MS1-H13 hybrid joints, where the fracture always occurred at the interface, and for MS1-C300 hybrid joints, which failed in the AM portion [29,30]. It was argued by Azizi [29] and Cyr [30] that fractures at the interface are caused by steep microstructure gradients and gradients of chemical composition. Both were documented in the MS1 maraging steel – CMnAlNb AHSS steel joint where they have not turned out to be critical for fracture. Earlier reports also mentioned the lower quality of dissimilar joints. The reason for different fracture behaviours of hybrid parts might be in the different qualities of the joints produced in various facilities. This aspect is worth further investigation because it could result in an improved joint performance. At this point, it is rather difficult to compare the production conditions between different facilities due to a lack of details in respective publications.

Different fracture morphologies can be found in scanning electron

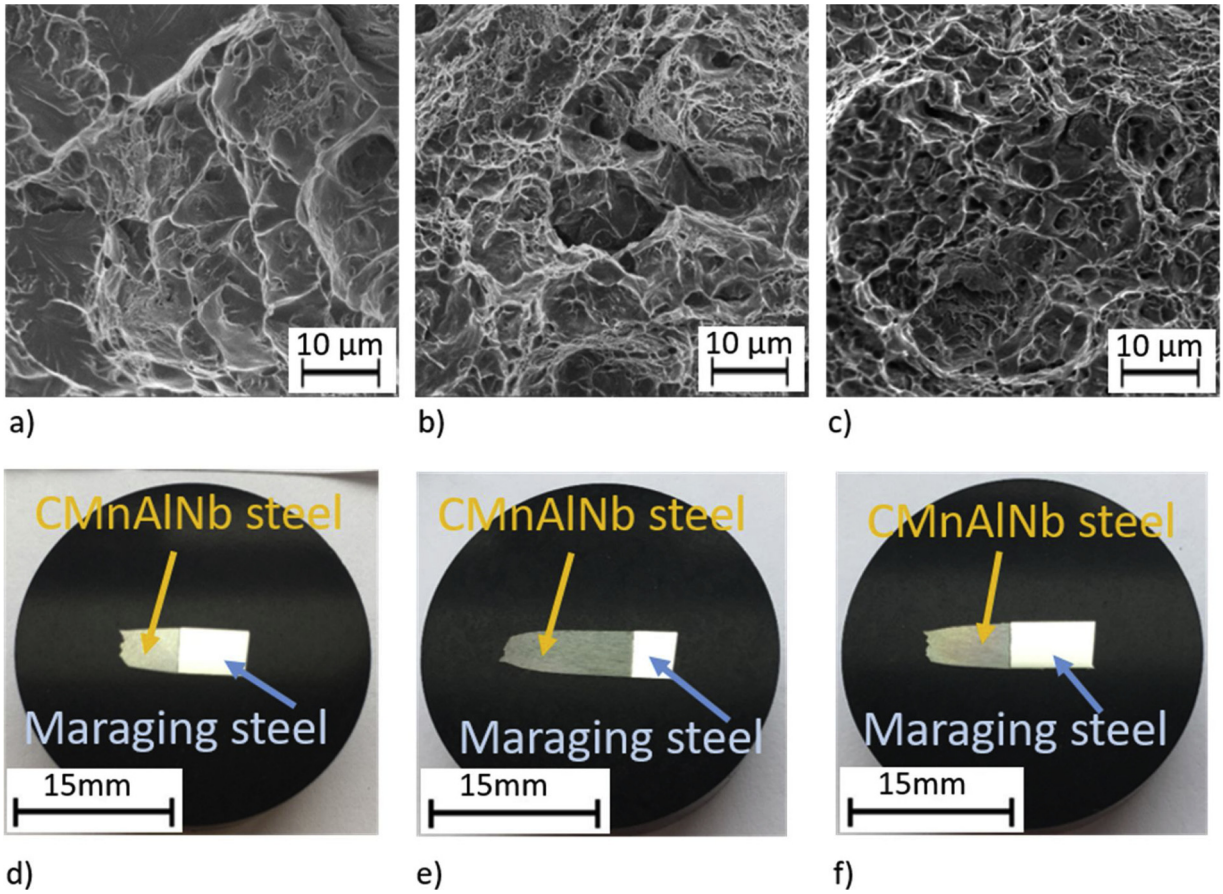

Fig. 12. Fracture surfaces (a–c) and longitudinal metallographic sections of fractured samples (d–f) of samples with different post-AM heat treatments: Sample 1- CMnAlNb without HT, no post-build HT a), d); Sample 4 – CMnAlNb without HT, post-build two-step HT 900 °C/20 min, 425 °C/60 min b), e); sample 6 - CMnAlNb 900 °C/20 min - 425 °C/20 min, post-build annealed 200 °C/120 min c), f).

micrographs (Fig. 12). In the first sample without prior or post-build heat treatment, the fracture surface had a mixed brittle-ductile appearance (Fig. 12a). Many distinctive brittle fracture facets were observed among ductile areas with a dimple morphology. The occurrence of brittle fracture can be attributed to the presence of pearlite in the forged CMnAlNb steel without heat treatment. A similar fracture with fewer brittle fracture areas was found in sample 2 (post-build annealed at 900 °C), where CMnAlNb steel still contained a small amount of pearlite. Samples with pre-AM heat treatment of CMnAlNb steel alone and samples with various post-AM heat treatments fractured in a ductile manner, showing dimples of various sizes and parts of broken AlN particles still visible at the bottom of many dimples (Fig. 12b, c).

4. Conclusions

Hybrid parts were additively manufactured by depositing maraging steel on a cylindrical semi-product of conventional CMnAlNb high-strength steel. It should be noted that this production of hybrid parts by SLM technology requires precise adjustment of the semi-product at the base plate and flat vertical top surface of used semi-products to ensure successful deposition. Various heat treatments of CMnAlNb steel prior to additive manufacturing were carried out and different heat treatments were then applied to hybrid parts. The purpose was to study the effects of pre and post-build heat treatment on the mechanical properties of the hybrid part.

CMnAlNb steel had lower strength and higher ductility than the maraging steel, regardless of heat treatment. Yet, all the hybrid parts exhibited higher strengths than CMnAlNb steel and slightly higher total elongation than the maraging steel alone. The best combination of ultimate tensile strength, 862 MPa, and total elongation, 19 %, was obtained in a hybrid part after pre-build two-step heat-treatment of CMnAlNb steel, and with no post-build heat treatment. All hybrid parts fractured in the CMnAlNb steel portion, several millimetres from the interface.

CRediT authorship contribution statement

Ludmila Kučerová: Conceptualization, Methodology, Visualization, Supervision, Writing - original draft, Writing - review & editing. **Ivana Zetková:** Methodology, Investigation, Writing - original draft. **Štěpán Jeníček:** Methodology, Investigation. **Karolína Burdová:** Investigation, Writing - review & editing.

Declaration of Competing Interest

The authors declare that there are no conflicts of interest.

Acknowledgements

The present contribution has been prepared under project ITI CZ.02.1.01/0.0/0.0/18_069/0010040, “Research of additive technologies for future application in mechanical engineering practice – RTI plus” under the auspices of the National Sustainability Programme I of the Ministry of Education of the Czech Republic aimed to support research, experimental development and innovation.

References

[1] K. Kempen, E. Yasa, L. Thijs, et al., Microstructure and mechanical properties of selective laser melted 18Ni-300 steel, Phys. Procedia 12 (2011) 255–263.
[2] Y. Bai, Y. Yang, D. Wang, et al., Influence mechanism of parameters process and mechanical properties evolution mechanism of maraging steel 300 by selective laser melting, Mater. Sci. Eng. A 703 (2017) 116–123.
[3] T.H. Simm, L. Sun, D.R. Galvin, et al., The effect of a two-stage heat-treatment on the microstructural and mechanical properties of a maraging steel, Materials 10 (2017) 1346.
[4] J. Mutua, S. Nakata, T. Onda, et al., Optimization of selective laser melting parameters and influence of post heat treatment on microstructure and mechanical properties of maraging steel, Mater. Des. 139 (2017) 486–497.
[5] Ch. Tan, K. Zhoua, W. Ma, et al., Microstructural evolution, nanoprecipitation behavior and mechanical properties of selective laser melted high-performance grade 300 maraging steel, Mater. Des. 134 (2017) 23–34.
[6] B. Mooney, K.I. Kourousis, R. Raghavendra, Plastic anisotropy of additively manufactured maraging steel: influence of the build orientation and heat treatments, Addit. Manuf. 25 (2019) 19–31.
[7] L. Kučerová, I. Zetková, A. Jandová, M. Bystrianský, Microstructural characterisation and in-situ straining of additive-manufactured X3NiCoMoTi 18-9-5 maraging steel, Mater. Sci. Eng. A 750 (2019) 80–90.
[8] N. Li, S. Huang, G. Zhang, et al., Progress in additive manufacturing on new materials: a review, J. Mater. Sci. Technol. 35 (2019) 242–269.
[9] T.D. Ngo, A. Kashani, G. Imbalzano, et al., Additive manufacturing (3D printing): a review of materials, methods, applications and challenges, Compos. Part B Eng. 143 (2018) 172–196.
[10] J. Faludi, C.M. Van Sice, Y. Shi, J. Bower, O.M.K. Brooks, Novel materials can radically improve whole-system environmental impacts of additive manufacturing, J. Clean. Prod. 212 (2019) 1580–1590.
[11] D. Bourell, J.P. Kruth, M. Leu, et al., Materials for additive manufacturing, CIRP Ann. Manuf. Technol. 66 (2017) 659–681.
[12] L. Kučerová, I. Zetková, Metallography of 3D printed 1.2709 tool steel, Manuf. Technol. 16 (1) (2016) 140–144.
[13] E.A. Jägle, Z. Sheng, P. Kurnsteiner, et al., Comparison of maraging steel Micro- and nanostructure produced conventionally and by laser additive manufacturing, Materials 10 (2017) 1–15.
[14] M. Monkova, I. Zetkova, L. Kučerová, et al., Study of 3D printing direction and effects of heat treatment on mechanical properties of MS1 maraging steel, Arch. Appl. Mech. (2018) 1–14.
[15] S. Yin, C. Chen, X. Yan, X. Feng, R. Jenkins, P. O'Reilly, M. Liu, H. Li, R. Lupoi, The influence of aging temperature and aging time on the mechanical and tribological properties of selective laser melted maraging 18Ni-300 steel, Addit. Manuf. 22 (2018) 592–600.
[16] P. Kürnsteiner, M.B. Wilms, A. Weisheit, et al., In-process precipitation during laser additive manufacturing investigated by atom probe tomography, Microsc. Microanal. 23 (1) (2017) 694–695.
[17] Y. Zhang, A. Bandyopadhyay, Direct fabrication of bimetallic Ti6Al4V + Al12Si structures via additive manufacturing, Addit. Manuf. 29 (2019) 100783.
[18] S. Yin, X. Yan, C. Chen, R. Jenkins, M. Liu, R. Lupoi, Hybrid additive manufacturing of Al-Ti6Al4V functionally graded materials with selective laser melting and cold spraying, J. Mater. Process. Tech. 255 (2018) 650–655.
[19] V.K. Balla, P.D. Devasconcellos, W. Xue, Fabrication of compositionally and structurally graded Ti – TiO 2 structures using laser engineered net shaping (LENS), Acta Biomater. 5 (2009) 1831–1837.
[20] H. Sahasrabudhe, J. Soderlind, A. Bandyopadhyay, Laser processing of in situ TiN/Ti composite coating on titanium, J. Mech. Behav. Biomed. Mater. 53 (2016) 239–249.
[21] B. Onuike, A. Bandyopadhyay, Additive manufacturing of Inconel 718 – Ti6Al4V bimetallic structures, Addit. Manuf. 22 (2018) 844–851.
[22] J.S. Zuback, T.A. Palmera, T. DebRoy, Additive manufacturing of functionally graded transition joints between ferritic and austenitic alloys, J. Alloys Compd. 770 (2019) 995–1003.
[23] H. Hur, K. Lee, Zhu-hu, J. Kim, Hybrid rapid prototyping system using machining and deposition, Comput. Aided Des. 34 (2002) 741–754.
[24] P. Stavropoulos, P. Foteinopoulos, A. Papacharalampopoulos, H. Bikas, Addressing the challenges for the industrial application of additive manufacturing: towards a hybrid solution, Int. J. Lightweight Mater. Manuf. 1 (2018) 157–168.
[25] W. Du, Q. Bai, B. Zhang, A novel method for additive/subtractive hybrid manufacturing of metallic parts, Procedia Manuf. 5 (2016) 1018–1030.
[26] G. Ambrogio, F. Gagliard, M. Muzzupappa, L. Filice, Additive-incremental forming hybrid manufacturing technique to improve customised part performance, J. Manuf. Process. 37 (2019) 386–391.
[27] C. Luo, Y. Zhang, Fusion zone characterization of resistance spot welded maraging steels via selective laser melting, J. Mater. Process. Tech. 273 (2019) 11653.
[28] M.D. Bambach, M. Bambach, A. Sviridov, S. Weiss, New process chains involving additive manufacturing and metal forming – a chance for saving energy? Procedia Eng. 207 (2017) 1176–1181.
[29] H. Azizi, R. Ghiaasiaan, R. Prager, M.H. Ghoncheh, K.A. Samk, A. Lausic, W. Byleveld, A.B. Phillion, Metallurgical and mechanical assessment of hybrid additively-manufactured maraging tool steels via selective laser melting, Addit. Manuf. 27 (2019) 389–397.
[30] E. Cyr, H. Asgari, S. Shamsdini, M. Purdy, K. Hosseinkhani, M. Mohammadi, Fracture behaviour of additively manufactured MS1-H13 hybrid hard steels, Mater. Lett. 212 (2018) 174–177.
[31] L.M.S. Santos, J. Jesus, J.M. Ferreirea, J.D. Costa, C. Capela, Fracture toughness of hybrid components with selective laser melting 18Ni300 steel parts, Appl. Sci. Basel (Basel) 8 (2018) 1879.
[32] B.C. De Cooman, Structure-properties relationship in TRIP steels containing carbide-free bainite, Curr. Opin. Solid State Mater. Sci. 8 (2004) 285–303.
[33] L. Kučerová, K. Opatová, J. Káňa, H. Jirková, High versitality of niobium alloyed AHSS, Arch. Metall. Mater. 62 (3) (2017) 1485–1491.
[34] J. Chiang, J.D. Boyd, A.K. Pilkey, Effect of microstructure on retained austenite stability and tensile behaviour in an aluminum-alloyed TRIP steel, Mater. Sci. Eng. A 638 (2015) 132–142.
[35] J.N. Huang, Z.Y. Tang, H. Ding, R.D.K. Misra, The significant impact of phase fraction and austenite stability on the mechanical properties of a low-alloyed TRIP-aided steel: an insight into experimental analysis and predictions, Mater. Sci. Eng. A 759 (2019) 40–46.
[36] L. Kučerová, The effect of two-step heat treatment parameters on microstructure and mechanical properties of 42SiMn steel, Metals 7 (12) (2017) 1–14.
[37] Y.F. Shen, L.N. Qiu, Sun X, et al., Effects of retained austenite volume fraction, morphology, and carbon content on strength and ductility of nanostructured TRIP-assisted steels, Mater. Sci. Eng. A 636 (2015) 551–564.
[38] J. Zhao, X. Zhao, X. Zhao, C. Dong, S. Kang, Eff ;ects of nucleation site and morphology of carbide-free bainite on microstructures and properties of bainite/martensite multi-phase steels, Mater. Sci. Eng. A 744 (2019) 86–93.
[39] L. Kučerová, H. Jirková, B. Mašek, Influence of Nb micro-alloying on TRIP steels treated by continuous cooling process, Manuf. Technol. 16 (1) (2016) 145–149.
[40] T.K. Han, S.S. Park, K.H. Kim, C.Y. Kang, I.S. Woo, J.B. Lee, CO2 laser welding characteristics of 800 MPa class TRIP steel, ISIJ Int. 45 (2005) 60–65.
[41] R.S. Sharma, P. Molian, Yb:YAG laser welding of TRIP780 steel with dual phase and mild steels for use in tailor welded blanks, Mater. Des. 30 (2009) 4146–4155.
[42] N. Lun, D.C. Saha, A. Macwan, H. Pan, L. Wang, F. Goodwin, Y. Zhou, Microstructure and mechanical properties of fibre laser welded medium manganese, TRIP steel, Mater. Des. 131 (2017) 450–459.
[43] A. Grajcar, M. Rózañski, M. Kamiñska, B. Grzegorczyk, Effect of gas atmosphere on the non-metallic inclusions in laser-welded trip steel with Al and Si additions, Mater. Tehnol. 50 (2016) 945–950.
[44] M.H. Razmpoosh, A. Macwan, E. Biro, Y. Zhou, Microstructure and dynamic tensile characteristics of dissimilar fiber laser welded advanced high strength steels, Mater. Sci. Eng. (2020) Article in Press.
[45] L. Kučerová, M. Bystrianský, Comparison of thermo-mechanical treatment of C-Mn-Si-Nb and C-Mn-Si-Al-Nb TRIP steels, Procedia Eng. 207 (2017) 1856–1861 Cambridge: Elsevier Ltd.
[46] L. Kučerová, H. Jirková, B. Mašek, Continuous cooling of CMnSi TRIP steel, Mater. Today Proc. 2 (2015) 677–680. Amsterodam: Elsevier Ltd.
[47] S.S. Nayaka, V.H.B. Hernandeza, Y. Okitaa, Y. Zhou, Microstructure–hardness relationship in the fusion zone of TRIP steel welds, Mater. Sci. Eng. A 551 (2012) 73–81.
[48] J.J. Guzman-Aguilera, et al., Influence of SC-HAZ microstructure on the mechanical behavior of Si-TRIP steel welds, Mater. Sci. Eng. A 718 (2018) 216–227.